A low-cost method to measure the timing of postfire flash floods and debris flows relative to rainfall

Jason W. Kean,[1] Dennis M. Staley,[1] Robert J. Leeper,[2] Kevin M. Schmidt,[3] and Joseph E. Gartner[1]

Received 28 September 2011; revised 23 March 2012; accepted 23 March 2012; published 9 May 2012.

[1] Data on the specific timing of postfire flash floods and debris flows are very limited. We describe a method to measure the response times of small burned watersheds to rainfall using a low-cost pressure transducer, which can be installed quickly after a fire. Although the pressure transducer is not designed for sustained sampling at the fast rates ($\leq$2 s) used at more advanced debris flow monitoring sites, comparisons with high-frequency stage data show that measured spikes in pressure sampled at 1 min intervals are sufficient to detect the passage of most debris flows and floods. Postevent site visits are used to measure the peak stage and identify flow type on the basis of deposit characteristics. The basin response time scale (t_b) to generate flow at each site was determined from an analysis of the cross correlation between time series of flow pressure and 5 min rainfall intensity. This time scale was found to be less than 30 min for 40 postfire floods and 11 postfire debris flows recorded in 15 southern California watersheds ($\leq$1.4 km^2). Including data from 24 other debris flows recorded at 5 more instrumentally advanced monitoring stations, we find there is not a substantial difference in the median t_b for floods and debris flows (11 and 9 min, respectively); however, there are slight, statistically significant differences in the trends of flood and debris flow t_b with basin area, which are presumably related to differences in flow speed between floods and debris flows.

Citation: Kean, J. W., D. M. Staley, R. J. Leeper, K. M. Schmidt, and J. E. Gartner (2012), A low-cost method to measure the timing of postfire flash floods and debris flows relative to rainfall, *Water Resour. Res.*, *48*, W05516, doi:10.1029/2011WR011460.

1. Introduction

[2] Steep, recently burned watersheds are vulnerable to flash floods and debris flows. Combined data on the rainfall and relative timing of postfire runoff are important for calibration and testing of rainfall-runoff models and constraining the hydrologic triggering conditions of postfire floods and debris flows. Despite its importance, limited data on postfire flood and debris flow timing exist because of challenges presented by the infrequent occurrence, steep terrain, destructive potential, and short lead time available to instrument new sites. Rare time series of postfire runoff have come from either preexisting streamflow gaging stations located in or near the burn area [e.g., *Scott*, 1993; *Moody and Martin*, 2001; *McLin et al.*, 2001; *Lane et al.*, 2006; *Cydzik and Hogue*, 2009], or from installation of new monitoring sites after fires, such as those designed to measure streamflow [e.g., *Robichaud*, 2005; *Moody et al.*, 2008], suspended sediment [e.g., *Malmon et al.*, 2007; *Smith et al.*, 2011], hillslope runoff [e.g., *Wilson*, 1999; *Sheridan et al.*, 2007; *Kinner and Moody*, 2010; *Robichaud et al.*, 2010; *Schmidt et al.*, 2011], and debris flows [*Kean et al.*, 2011]. Presently, however, there is little overlap in the spatial scales for which postfire flood and debris flow data have been collected, making it difficult to compare time series of floods and debris flows in comparable sized basins.

[3] Here, in an effort to expand collection of postfire flow data, we describe a low-cost method to measure the response times of flash floods and debris flows in small watersheds. Our approach uses a readily available pressure transducer designed to monitor groundwater levels and stage in low-gradient streams. The method requires a small amount of easily portable equipment and is thus well suited for rapidly establishing a network of timing stations in the often short time period between the end of a fire and the first rain storm. When paired with rainfall data and postevent field observations of flow type and peak depth, the timing data document the hydrologic conditions of an event at a level of detail only surpassed by more advanced (and expensive) monitoring sites. We first evaluate the method for both floods and debris flows at more instrumentally advanced sites equipped with noncontact stage gauges. We then present examples from application of the method to 15 sites in recently burned areas of southern California. Finally, we use data collected from these sites to investigate an important question regarding postfire hazards: What is the difference in basin response times between postfire flash floods and postfire debris flows?

[1]U.S. Geological Survey, Denver, Colorado, USA.
[2]U.S. Geological Survey, Pasadena, California, USA.
[3]U.S. Geological Survey, Menlo Park, California, USA.

Table 1. Sensor Specifications

Measurement	Make and Model[a]	Sampling Rate	Accuracy/Resolution	Sites
Pressure (nonvented)	Solinst Model 3001	1 min	±5 mm/1 mm (water depth)	Low-cost sites[b]
Precipitation	Texas Electronics TR525	Every bucket tip	±1%/0.2 mm	Low-cost sites
Pressure (vented)	Campbell Scientific CS450	2 s	±5 mm/1 mm (water depth)	Arroyo Seco, Dunsmore 1
Stage (laser)	SICK DT50-HI	10 Hz	±7 mm/1 mm	Arroyo Seco, Dunsmore 1
Stage (radar)	Endress + Hauser M FMR250	30 s	±3 mm/1 mm	Winter 4

[a]Any use of trade, product, or firm names is for descriptive purposes only and does not imply endorsement by the U.S. Government.
[b]Low-cost sites include all but the last five sites listed in Table 2.

2. Measurement Methods

[4] The timing of the passage of floods and debris flows was identified from peaks in pressure readings made using nonvented pressure transducers (Table 1). The small sensor (2.2 cm by 15 cm) has a self-contained data logger and power supply, and a maximum pressure head range of 15 m. The pressure transducers were installed in holes (16 cm deep by 2.5 cm in diameter) drilled vertically into exposed bedrock sections of the channel bed using a battery-powered hammer drill. The orifice of the pressure transducer was positioned 1 cm below the bedrock surface and covered with a mesh screen (0.5 mm opening; 0.1 mm wire) to inhibit clogging by sediment. A wire loop was attached to the sensor to aid in removing it from the hole for data retrieval. The limited exposure of the sensor to the flow, and lack of external data/power cables, increased the chances of survival during large events; however four sensors were lost to bedrock erosion by debris flows. A metal detector was used to locate pressure transducers buried by sediment. Photographs of the sensor, installation, and maintenance of the sites are shown in Figure S1 of the auxiliary material.[1]

[5] The sampling rate of the pressure transducer was restricted by the limited memory of the onboard data logger (40,000 records), but the data logger could be programmed to either stop recording once the memory was full, or continue logging by overwriting the oldest records (ring mode). Our project included sites that were difficult to access and staff members stationed far from the monitoring areas. For this reason, a 1 sample per minute rate, which takes 27.7 days to fill/overwrite the memory, was identified as the minimum practical rate for maintaining our network of timing stations. Although the 1 min rate was not adequate to resolve the details of pressure fluctuations associated with fast-moving debris flows [e.g., *McArdell et al.*, 2007], it was sufficient to detect the timing of these events to within a few minutes, as well as resolve the shape of gradually varying flood hydrographs. As will be shown in section 3, a sampling rate of 2 s provides a much better representation of the pressure near the time of peak debris flow. Monitoring at the 2 s rate is possible using the ring mode of the pressure transducer; however, it would only be practical for a project with staff stationed very close to the sites, because there is only 22 h to recover the data after an event before they are overwritten.

[6] We installed the pressure transducers at the outlets of 15 small basins ($\leq$1.4 km^2) in four different mountain ranges in southern California (Table 2). The basins were burned by fires between 2006 and 2009. Data were collected in the first winter after the fire, with the exception of the three Ruby sites, where data collection took place in the second year after fire following an exceptionally dry first year. The sites were on ephemeral channels, and the pressure record was corrected for atmospheric pressure by subtracting the recorded pressure at the beginning of each rain storm before flow occurred. We did not adjust the pressure record for atmospheric pressure deviations that occurred after the start of each storm; however, such deviations could be removed using a separate pressure transducer as a barometer. A tipping bucket rain gauge was installed in or near the basin of each pressure transducer, and the cross section at each pressure transducer was surveyed using a total station.

[7] Field visits to the sites were made following each storm to download data, survey high-flow marks, and examine flow deposits to determine the type of flow. Flows were classified as debris flows if unsorted, unstratified, and matrix-supported deposits or mud veneers were observed in the channel and/or fan apex near the sensor. If these features were not observed, the events were classified as floods (both water and sediment laden). This classification scheme assumes that debris flows must have a higher stage than subsequent water floods to be preserved. Identification of the type of flow based on postevent observations was necessary because the pressure data by itself cannot distinguish between debris flows, sediment-laden floods, and water floods because of the unknown flow density and the effects of flow dynamics on measured pressure. Identifying these types of flows during an event requires more sophisticated instrumentation, such as that designed to measure flow density [*McArdell et al.* 2007] or ground vibrations [*LaHusen*, 2005]. Similarly, surveys of high-flow marks were required to determine the peak flow depth, because peak flow depth and peak pressure head will only correspond in the special case of hydrostatic flow.

[8] To assess our method of detecting the timing of floods and debris flows with pressure transducers, we compared time series of pressure and flow stage at sites that were also equipped with noncontact stage gauges (Tables 1 and 2). Five of these sites (Arroyo Seco, Dunsmore 1 and 2, Big Tujunga, and Jesusita) are described in detail by *Kean et al.* [2011]. At those sites stage was measured using either laser or ultrasonic distance meters that were suspended above vented pressure transducers mounted in the channel bed. The vented pressure transducers were connected to external data loggers and sampled at a much faster rate than the nonvented pressure transducers used at

[1]Auxiliary materials are available in the HTML. doi:10.1029/2011WR011460.

Table 2. Summary of Site Characteristics

Site	Range	Fire	Northing/Easting[a] (UTM)	Basin Area Above Sensor (ha)	Maximum/Minimum Elevation[b] (m)	50th/90th Percentile Basin Slope[b] (deg)	Peak Flow Type[c]
Ruby 1	Whitaker Peak	2006 Day	3828702/340934	9.2	1222/1051	32/38	F
Ruby 2	Whitaker Peak	2006 Day	3828296/340826	30	1222/895	34/41	F
Ruby 3	Whitaker Peak	2006 Day	3828265/340768	130	1222/885	34/41	F
Winter 1	Santa Monica	2007 Canyon	3768525/342832	0.7	352/278	34/42	F
Winter 2	Santa Monica	2007 Canyon	3768352/342837	14	424/232	31/41	F
Winter 3	Santa Monica	2007 Canyon	3768176/342889	22	424/150	33/44	F
Winter 4[d]	Santa Monica	2007 Canyon	3767822/342848	39	424/93	33/45	F
Wylie 1	Santa Ynez	2008 Gap	3818484/238407	0.9	232/134	36/45	F
Wylie 2	Santa Ynez	2008 Gap	3818471/238366	5.7	253/114	35/45	F
Gould	San Gabriel	2009 Station	3788019/390058	33	991/630	43/53	DF
Mullally	San Gabriel	2009 Station	3789635/387744	63	1288/767	41/52	DF
Oak	San Gabriel	2009 Station	3790460/385448	1.9	915/749	43/53	DF
Shields	San Gabriel	2009 Station	3790540/386075	38	1366/817	40/52	DF
Starfall	San Gabriel	2009 Station	3790279/386217	29	1317/762	39/51	DF
Winery	San Gabriel	2009 Station	3788352/389060	18	989/684	41/51	DF
Arroyo Seco[e]	San Gabriel	2009 Station	3788964/389956	1.4	1040/940	39/46	DF
Big Tujunga [e]	San Gabriel	2009 Station	3794688/386462	140	1548/571	38/48	DF
Dunsmore 1[e]	San Gabriel	2009 Station	3791625/385649	48	1548/989	38/51	DF
Dunsmore 2[e]	San Gabriel	2009 Station	3790898/385225	11	1149/784	39/50	DF
Jesusita[e]	Santa Ynez	2009 Jesusita	3817186/251989	2.2	540/429	30/36	DF

[a]Zone 11, NAD83.
[b]From a 1 m digital elevation model (DEM) except at Jesusita, which is from a 10 m DEM.
[c]F, flood; DF, debris flow.
[d]Site with stage gauge.
[e]*Kean et al.* [2011] sites with stage gauges.

the low-cost sites (2 s versus 1 min). The vented pressure transducer at Dunsmore 1 was destroyed by a debris flow on 18 January 2010 and was replaced with a nonvented pressure transducer. Stage at a sixth site (Winter 4) was measured using a radar distance meter that was located 2.5 m upstream of a nonvented transducer.

3. Example Measurements

3.1. Comparison of Pressure Head and Flow Stage

[9] We first present examples of pressure head (P) and flow stage (H) measured at the instrumentally more advanced sites equipped with both pressure transducers and noncontact stage gauges (Figure 1). These examples demonstrate the ability of the pressure transducer to detect flow timing, but also illustrate the limitations of interpreting the magnitude of the pressure signal. The first example (Figure 1a) shows a flood having a nearly hydrostatic pressure on the basis of the similarity between pressure head (sampled at 1 min) and flow stage (sampled at 30 s) measured 2.5 m upstream at a slightly wider cross section. In cases of hydrostatic flow, the time series of pressure head is equivalent to water flow depth and, thus, could be converted to an indirect estimate of discharge using an appropriate flow model of the site. Although nearly hydrostatic pressure was present at several of our sites as will be described in section 3.2, water flow in steep channels cannot, in general, be assumed to be hydrostatic [*Denlinger and O'Connell*, 2008]. An example of a flood with nonhydrostatic pressure is given in Figure 1b. There peaks in pressure head (sampled at 2 s) greatly exceed the flow stage (sampled at 10 Hz). Although the time series of pressure head in this example is not suitable for estimating flow depth and discharge, the peaks in pressure, which coincide with an increase in rainfall intensity [see *Kean and Staley*, 2011], correctly identify the time of peak flow. As shown by the red triangles in Figure 1b, the timing of this flood could have been resolved adequately using a slower sampling rate of 1 min.

[10] High pore pressures are often generated at the base of debris flows and greatly contribute to their mobility [*Iverson*, 1997; *McArdell et al.*, 2007]. As shown in Figures 1c and 1d, measured spikes in pore pressure can be used to detect when a debris flow passes the cross section [see also *Kean and Staley*, 2011; *Kean et al.*, 2011]. Like nonhydrostatic floods, however, the magnitude of the debris flow pressure signal cannot be easily related to flow stage because of the complex flow dynamics of debris flows and unknown density. In addition, the magnitude of the pressure signal generated by a debris flow can be damped if the sensor is covered by a partially saturated layer of sediment [e.g., *McCoy et al.*, 2010; *Berger et al.*, 2011; *Kean and Staley*, 2011].

[11] The rapid stage changes associated with the small debris flow shown in Figure 1c highlights the need for fast sampling rates for detection. The 2 s sampling rate (continuous orange line) captures the excess pore pressure generated by the first steep-fronted surge, while the 1 min subsample of pressure (red triangles), which is used to simulate the slow sampling rates we used for the nonvented pressure transducers, misses the spike in pressure. While not ideal, the slow 1 min rate does, however, detect the rise in pressure associated with the tail of the second surge about 3 min later. For the larger and longer-duration debris flow shown in Figure 1d, a 1 min sampling of rate of pressure (continuous orange line) clearly identifies the timing of flow, though details of the pressure fluctuations are unresolved.

3.2. Measurements of Flood and Debris Flow Pressure at Low-Cost Stations

[12] Here we present representative examples of floods (Figure 2) and debris flows (Figure 3) recorded at the

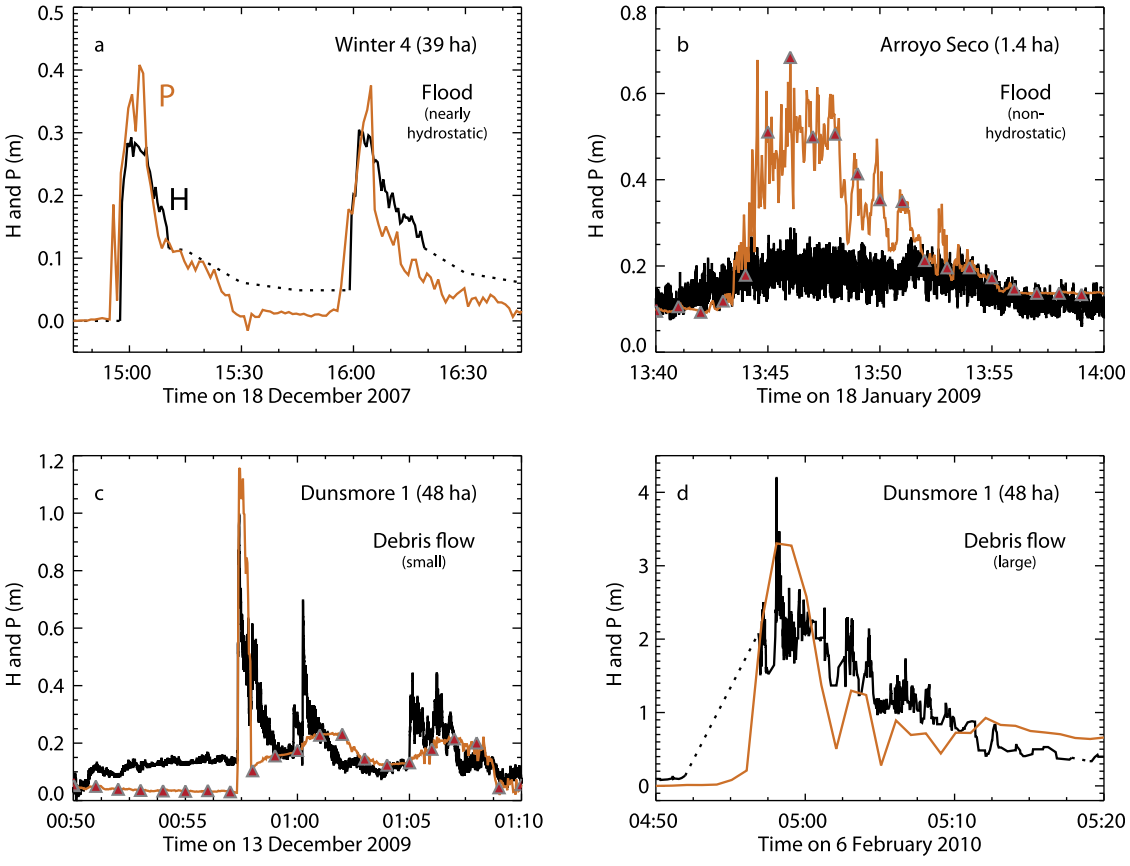

Figure 1. Examples of pressure head (P, orange) and flow stage (H, black) during (a and b) two floods and (c and d) two debris flows. The datum for H is the elevation of the pressure transducer. H in Figure 1a was measured using a radar distance meter suspended above a cross section 2.5 m upstream of the pressure transducer; H in Figures 1b–1d was measured using laser distance meters suspended above the pressure transducer. Dashed portions of the stage record in Figures 1a and 1d correspond to periods where the sampling interval exceeded 2 min. P in Figures 1a and 1d was recorded at 1 min intervals using a nonvented pressure transducer. P in Figures 1b and 1d was recorded at 2 s intervals using a vented pressure transducer; the red triangles in Figures 1b and 1c are subsamples of the record at 1 min intervals.

low-cost sites equipped with only a nonvented pressure transducer and rain gauge. These examples provide further guidance on interpreting the pressure measurements and reveal differences in flow timing relative to drainage area. Figures 2 and 3 show measured pressure head (P), storm cumulative rainfall (R), 5 min rainfall intensity (I_5), and, when available, peak flow stage (H_p) surveyed after the event. Sites are grouped in pairs that share a common rain gauge. The paired flood sites are nested within the same drainage basin; the paired debris flow sites are in adjacent basins. Figures 2 (left) and 3 (left) show P and R during the entire storm, while Figures 2 (right) and 3 (right) show the details of P and I_5 during 1 h around the time of peak flow. Pressure head in Figures 2 (right) and 3 (right) is normalized by the maximum pressure head (P_{max}) to facilitate comparison between the timing of flow at paired sites of different size.

[13] Each of the flood examples in Figure 2 have a single distinct period of peak flow during the most intense rainfall of the storm. Measurements of peak stage (H_p) were made at three of the sites (Ruby 3, Winter 1, and Winter 4) and are within 12% of the measured peak pressure head. This agreement suggests that the flows at these sites have nearly hydrostatic pressure, and that discharge hydrographs could potentially be estimated indirectly. At Ruby 1, however, accurate indirect estimates of discharge can probably not be made for the period between 16:00 and 19:00 (Figure 2a). At that site a tree had fallen into the cross section, which we were not able to remove before the storm. The tree, which altered the stage-discharge relation, was not present after the flood and was presumably washed away at about 19:00, when there is an anomalous rapid drop in pressure.

[14] Examples where debris flow deposits were observed after the storm are shown in Figure 3. Unlike the flood examples, there are multiple, comparable-sized spikes in pressure during the storm. During long-duration storms in burned areas, it is not uncommon for the flow processes to vary over the course of the storm because of changes in sediment supply and rainfall intensity [*Kean and Staley*, 2011; *Kean et al.*, 2011]. Consequently, it is difficult to determine which of the multiple pressure spikes are associated with debris flows and which are associated with floods.

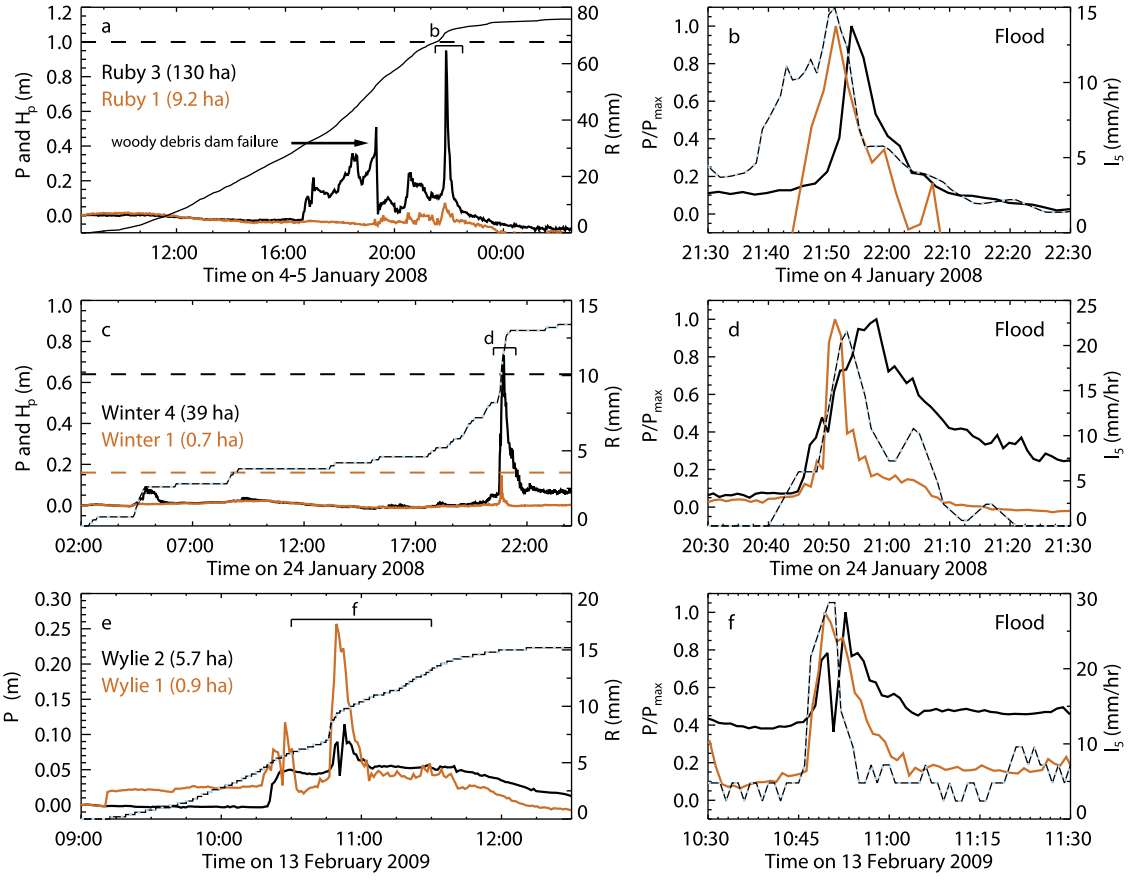

Figure 2. Examples of pressure head (P, solid lines) and rainfall measured during floods at low-cost sites. Sites are grouped in nearby pairs that share a common rain gauge. P for the larger drainage area site is plotted in black; P for the smaller of the two sites is plotted in orange. (a, c, e) P, storm cumulative rainfall (R, black/blue dotted line), and surveyed peak flow stage (H_p, horizontal dashed line). (b, d, f) P and 5 min rainfall intensity (I_5, black/blue dotted line) during 1 h around the time of peak flow. P in Figures 2b, 2d, and 2f is normalized by its maximum value P_{max}.

At nearby advanced monitoring sites equipped with stage gauges, similar multiple episodes of flow were recorded during the same storms [*Kean et al.*, 2011]. Most of these individual flow episodes were identified as debris flows on the basis of the stage records, which contained steep, high fronts characteristic of debris flow surges (e.g., Figures 1c and 1d). Unfortunately, a similar distinct signature of flow type is not always present in pressure records. This is especially true for the 1 min time series of pressure recorded at the low-cost sites, which is too coarse to resolve the rapid pressure increases associated with debris flow surges as shown in Figure 1. The measurements at Gould and Mullally (Figure 3c and 3e) provide additional examples of instances where the pressure during the surge was clearly under sampled. In those cases, surveyed peak flow stages ($H_p = 2.2$ at Gould and 4.1 m at Mullally) are substantially larger than measured peak pressure head ($\sim$1 m at both sites). We assume the field evidence of debris flows is associated with the peak pressure nearest in time to the peak rainfall intensity of the storm (Figure 3, right). In the absence of additional constraints on flow type, the type of flow during the other peaks in pressure is indeterminate.

[15] In some cases, however, such as the 6 February 2010 storm at Mullally (Figure 3e and 3f), additional observations can be used to identify the type of flows associated with the three pressure spikes labeled in Figure 3e. Ten minutes before the first spike at 3:27, a debris flow was recorded at a nearby advanced debris flow monitoring site (Arroyo Seco) 2.4 km away [*Kean et al.*, 2011]. At 4:25, Los Angeles County Department of Public Works (LADPW) employees monitoring the Mullally debris retention basin (100 m downstream of our pressure transducer) observed that the 7000 m^3 capacity basin, which was empty prior to the storm, was completely full. Given the rapid filling of the debris basin and the temporally coincident Arroyo Seco debris flow, it is likely that the first Mullally pressure spike was caused by a debris flow. During the second pulse of rain (Figure 3f), the LADPW employees heard a loud flow that overtopped the full debris basin. Other LADPW employees en route to the site observed a debris flow carrying cars and concrete Jersey barriers traveling down the road leading to the basin. This debris flow ($H_p = 4.1$ m at the pressure transducer site) damaged or destroyed over 40 homes below Mullally debris basin [*Lin et al.*, 2010]. Post-storm field evidence of a debris flow lobe deposited near the outlet of the Mullally debris basin suggests the third spike in pressure at 7:30 was also caused by a debris flow. Video footage by local residents show this flow had

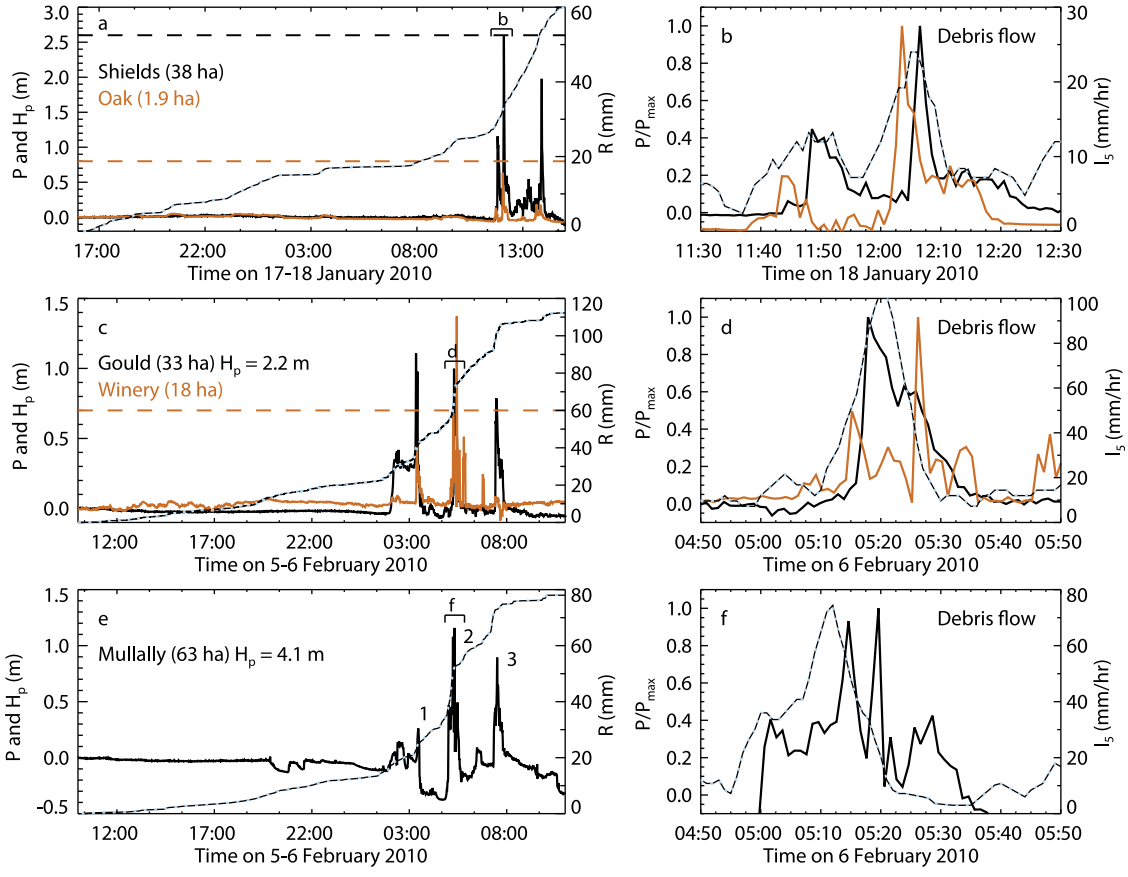

Figure 3. Representative examples of pressure head (solid lines) and rainfall (black/blue dotted lines) measured during debris flows at low-cost monitoring sites. Notation is the same as Figure 2. The three flow peaks labeled in Figure 3e are described in the text.

devolved to a sediment-laden flood by the time it reached the streets below the debris basin approximately 200 m downstream.

[16] Despite the difficulty of identifying flow type from pressure, and the limitations of relating pressure head to flow stage, spikes in pressure head are good indicators of flow timing. In all flood and debris flow examples of Figure 2 and 3, spikes in pressure head are closely associated with local increases in the rainfall intensity. This connection can be seen most clearly in the plots of I_5 and P/P_{max} shown in Figures 2 (right) and 3 (right). In all examples, maximum pressure occurs within minutes of the peak in rainfall intensity. Figures 2 (right) and 3 (right) also show slight differences in flow timing between paired sites having similar basin gradients, but different basin areas. With the exception of the Gould/Winery debris flow pair (Figure 3d), the peak pressure at the smaller site of each pair occurs a few minutes before the peak pressure of the larger site. At the Winery site (18 ha) the peak in pressure follows the peak at the larger Gould site (33 ha); however, the secondary peak at Winery, which is close to the measured peak stage, precedes the rise in pressure recorded at Gould.

4. Comparison of Flood and Debris Flow Timing

[17] To further investigate trends in flow timing relative to rainfall, basin area, and flow type, we calculated a measure of the time scale between rainfall and recorded postfire floods and debris flows. Only the 51 events that were clearly identified as either a flood or a debris flow are included in the analysis. A time scale between rainfall and flow at a station can be computed in several ways. The most common measure in hydrology is the lag time, which is defined as the time between the centroid of the rainfall distribution and the peak flow [*Sherman*, 1932]. While this time scale is well suited to address floods, it can sometimes be difficult to interpret for debris flows. The difficulty arises because the peak stage of debris flows can occur before the centroid of the rainfall distribution has accumulated [e.g., *Kean et al.*, 2011]. Similarly, the time of peak debris flow can also occur before the time of peak rainfall intensity. In their analysis of debris flow timing, *Kean et al.* [2011] attempted to avoid these complications by evaluating a basin response time scale (t_b) on the basis of the cross correlation between time series of flow stage and rainfall intensity. The cross correlation coefficient is a measure of the match in shape between two times series as a function of a time lag applied to one of them. *Kean et al.* [2011] defined the basin response time scale as $t_b = D - t_{lag}$, where D is the duration (5 min) over which rainfall intensity is computed ($I_D = [R(t) - R(t - D)]/D$), and t_{lag} is the time lag that maximizes the cross correlation coefficient for flow stage and rainfall intensity (i.e., the time lag that produces the best match in shape between flow stage and rainfall

intensity). The sign of t_{lag} is negative when the rainfall tends to precede the flow and positive when rainfall tends to follow the flow. The 5 min rainfall intensity was used because it was the rainfall intensity measure found to be best cross correlated with stage on the basis of an analysis of 24 recorded debris flows. In situations where the peak flow arrives after the centroid of rainfall distribution, the time scale t_b is very similar in value to the more commonly used lag time. In fact, the two time scales are nearly identical in the case of a symmetric rainfall distribution that precedes a symmetric hydrograph.

[18] Here we follow the approach of *Kean et al.* [2011] and compute the basin response time, t_b, for 40 floods and 11 debris flows using the measured time series of P and I_5 (Figure 4). We acknowledge that our values for debris flows may be biased by a few minutes toward longer times, because the slow 1 min sampling rate we used does not adequately resolve the initial rise in pressure associated with surge fronts. This bias, however, does not appear to significantly affect the results, because our values of t_b for debris flows (orange diamonds) compare favorably with the 24 values of t_b measured using high-frequency stage data collected at the nearby sites of *Kean et al.* [2011] (red diamonds).

[19] In general, the debris flows are associated with higher rainfall intensities than the floods, as indicated by the size of each flow symbol, which is scaled by the event 5 min peak rainfall intensity (I_{5p}). Interestingly, however, we find there is not a substantial difference in t_b between floods and debris flows. The median response times for floods and debris flows are 11 and 9 min respectively, and both sets of response times are lognormally distributed within a narrow half-hour range. Although the values of flood and debris flow t_b are very similar, the log-transformed mean of each population is likely statistically different (t test statistic = 2.4, significance = 0.019). These short response times demonstrate that there is only a short time for postfire flood or debris flow warning once intense rainfall begins. The similarity in timing of postfire floods and debris flows indicates that the recorded debris flows were likely generated by process related to surface water flow following intense bursts of rainfall rather than by hillslope failures caused by wetting of a slip surface from infiltration. This finding is consistent with both our field observations, which documented extensive rilling and channel erosion and very few meter-scale shallow landslide scars, and the observations of other postfire debris flow studies [*Meyer and Wells*, 1997; *Cannon et al.*, 2001; *Gabet and Bookter*, 2008; *Santi et al.*, 2008].

[20] With the exception of the three debris flow events circled in Figure 4, the response time scale for both floods and debris flows tend to increase with basin area as shown by the regression lines. *Kean et al.* [2011] suggested the three outlier events, which were small and associated with relatively low rainfall intensities, were likely very slow moving debris flows that lacked sufficient pore fluid pressures to overcome the flow resistance of the granular fronts. Despite some overlap between the flood and debris flow data, the slope of the regression lines are statistically different (residuals normally distributed, t test statistic = 3.09, significance = 0.001). The lower slope and position of the debris flow regression line relative to the flood trend, indicates that the debris flows tend to travel faster through the basin than floods. The difference in flow speed between debris flows and floods may be due to the greater peak flow

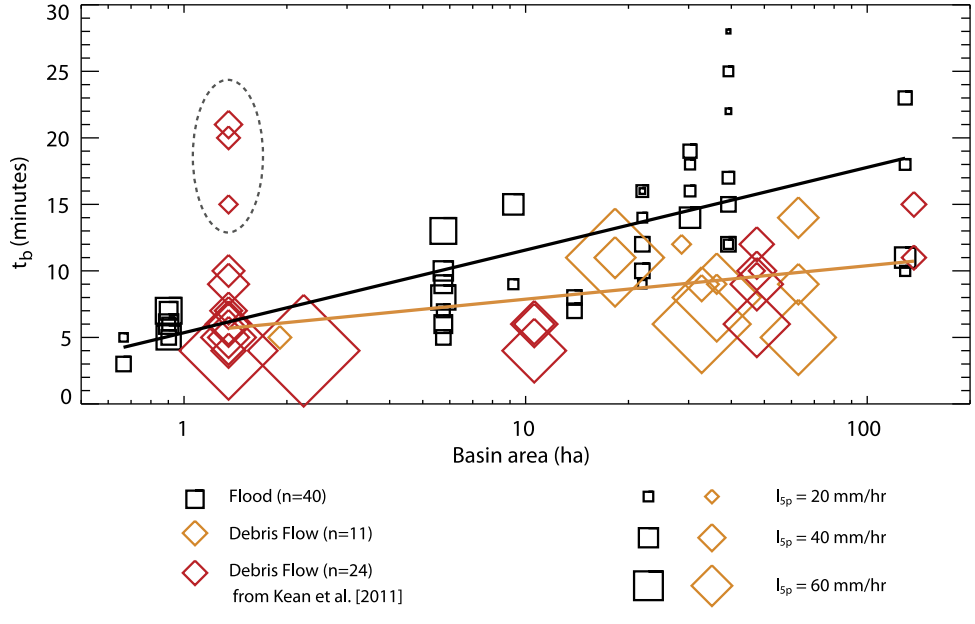

Figure 4. Basin response time (t_b) versus basin area for recorded floods (squares) and debris flows (diamonds). Orange diamonds are from low-cost pressure transducer sites, and red diamonds are from *Kean et al.* [2011]. The size of each symbol is scaled by the peak 5 min rainfall intensity (I_{5p}) near the time of peak stage. Regression lines for floods (r^2 = 0.51) and debris flows (r^2 = 0.37) are shown with the black and orange lines, respectively. The debris flow regression line does not include the three slow-moving debris flow events circled in the plot and described in the text.

depths of the debris flows than floods and the effects of high pore pressures on reducing the basal friction of debris flows [*Iverson et al.*, 2011].

5. Summary and Conclusions

[21] This study has shown that the timing of postfire flash floods and debris flows can be readily measured using a relatively inexpensive type of pressure transducer. The small sensor can be installed quickly in bedrock sections of channel, which are often present in small steep basins. Unlike trip wires, the sensor can record the timing of multiple flow events, which are common during long-duration storms in burned areas. Data collected using this technique, together with additional debris flow data of *Kean et al.* [2011], show there is not a substantial difference between when postfire floods and debris flows occur during a rainstorm. However, there are minor, statistically significant differences in the average response times of floods and debris flows relative to basin area that may be due to differences in flow speed between floods and debris flows. Although additional data might better define these trends, the data demonstrate that this simple approach is a viable low-cost method for measuring flow timing, which, together with rainfall data and postevent field observations of flow type and peak depth, provide rare constraints that can be used to help calibrate postfire rainfall-runoff models and identify the hydrologic triggering conditions of postfire debris flows. The approach may also be suitable for recording the timing of events in unburned settings.

[22] **Acknowledgments.** We thank Maiana Hanshaw, Alexander Woods, and Ryan Santos for field assistance and Susan Cannon, Paul Santi, Brian McArdell, Matteo Berti, and an anonymous reviewer for thoughtful reviews of this paper.

References

Berger, C., B. W. McArdell, and F. Schlunegger (2011), Direct measurement of channel erosion by debris flows, Illgraben, Switzerland, *J. Geophys. Res.*, *116*, F01002, doi:10.1029/2010JF001722.

Cannon, S. H., R. M. Kirkham, and M. Parise (2001), Wildfire-related debris-flow initiation processes, Storm King Mountain, Colorado, *Geomorphology*, *39*, 171–188.

Cydzik, K., and T. S. Hogue (2009), Modeling postfire response and recovery using the Hydrologic Engineering Center Hydrologic Modeling System (HEC-HMS), *J. Am. Water Resour. Assoc.*, *45*(3), 702–714, doi:10.111/j.1752-1688.2009.00317.x.

Denlinger, R. P., and D. R. H. O'Connell (2008), Computing nonhydrostatic shallow-water flow over steep terrain, *J. Hydraul. Eng.*, *134*(11), 1590–1602.

Gabet, E. J., and A. Bookter (2008), A morphometric analysis of gullies scoured by post-fire progressively-bulked debris flows in southwest Montana, USA, *Geomorphology*, *96*(3–4), 298–309.

Iverson, R. M. (1997), The physics of debris flow, *Rev. Geophys.*, *35*, 245–296.

Iverson, R. M., M. E. Reid, M. Logan, R. G. LaHusen, J. W. Godt, and J. P. Griswold (2011), Positive feedback and momentum growth during debris-flow entrainment of wet bed sediment, *Nat. Geosci.*, *4*, 116–121, doi:10.1038/ngeo1040.

Kean, J. W., and D. M. Staley (2011), Direct measurements of the hydrologic conditions leading up to and during post-fire debris flow in southern California, U.S.A., in *Debris-Flow Hazards Mitigation, Mechanics, Prediction, and Assessment*, edited by R. Genevois, D. L. Hamilton, and A. Prestininzi, pp. 685–694, Casa Ed. Univ. La Sapienza, Rome, doi:10.4408/IJEGE.2011-03.B-075.

Kean, J. W., D. M. Staley, and S. H. Cannon (2011), In situ measurements of post-fire debris flows in Southern California: Comparisons of the timing and magnitude of 24 debris-flow events with rainfall and soil moisture conditions, *J. Geophys. Res.*, *116*, F04019, doi:10.1029/2011JF002005.

Kinner, D. A., and J. A. Moody (2010), Spatial variability of steady-state infiltration into a two-layer soil system on burned hillslopes, *J. Hydrol.*, *381*, 322–332, doi:10.1016/j.jhydrol.200912.004.

LaHusen, R. (2005), Acoustic flow monitor system—User manual, *U.S. Geol. Surv. Open File Rep., 02-420*, 22 pp.

Lane, P. N. J., G. J. Sheridan, and P. J. Noske (2006), Changes in sediment loads and discharge from small mountain catchments following wildfire in south eastern Australia, *J. Hydrol.*, *331*, 495–510, doi:10.1016/j.jhydrol.2006.05.035.

Lin, R. G., V. Kim, and R. Vives (2010), 'Niagara' of mud hits homes: Dozens of houses in La Canada Flintridge are damaged or destroyed in a storm that defied forecast, *Los Angeles Times*, 7 Feb, A1, Los Angeles, CA.

Malmon, D. V., S. L. Reneau, D. Katzmann, A. Lavine, and J. Lyman (2007), Suspended sediment transport in an ephemeral stream following wildfire, *J. Geophys. Res.*, *112*, F02006, doi:10.1029/2005JF000459.

McArdell, B. W., P. Bartelt, and J. Kowalski (2007), Field observations of basal forces and fluid pore pressure in debris flow, *Geophys. Res. Lett.*, *34*, L07406, doi:10.1029/2006GL029183.

McCoy, S. W., J. W. Kean, J. A. Coe, D. M. Staley, T. A. Wasklewicz, and G. E. Tucker (2010), Evolution of a natural debris flow: In situ measurements of flow dynamics, video imagery, and terrestrial laser scanning, *Geology*, *38*(8), 735–738, doi:10.1130/G30928.1.

McLin, S. G., E. P. Springer, and L. J. Lane (2001), Predicting floodplain boundary changes following the Cerro Grande wildfire, *Hydrol. Processes*, *15*, 2967–2980.

Meyer, G. A., and S. G. Wells (1997), Fire-related sedimentation events on alluvial fans, Yellowstone National Park, U.S.A., *J. Sediment. Res.*, *67*(5), 776–791.

Moody, J. A., and D. A. Martin (2001), Post-fire, rainfall intensity–peak discharge relations for three mountainous watersheds in the western USA, *Hydrol. Processes*, *15*, 2981–2993, doi:10.1002/hyp.386.

Moody, J. A., D. A. Martin, S. L. Haire, and D. A. Kinner (2008), Linking runoff response to burn severity after a wildfire, *Hydrol. Processes*, *22*, 2063–2074, doi:10.1002/hyp.6806.

Robichaud, P. R. (2005), Measurement of post-fire hillslope erosion to evaluate and model rehabilitation treatment effectiveness and recovery, *Int. J. Wildland Fire*, *14*, 475–485.

Robichaud, P. R., J. W. Wagenbrenner, and R. E. Brown (2010), Rill erosion in natural and disturbed forests: 1. Measurements, *Water Resour. Res.*, *46*, W10506, doi:10.1029/2009WR008314.

Santi, P. M., V. G. deWolfe, J. D. Higgins, S. H. Cannon, and J. E. Gartner (2008), Sources of debris flow material in burned areas, *Geomorphology*, *96*, 339–354, doi:10.1016/j.geomorph.2007.02.022.

Schmidt, K. M., M. N. Hanshaw, J. F. Howle, J. W. Kean, D. M. Staley, J. D. Stock, and G. W. Bawden (2011), Hydrologic conditions and terrestrial laser scanning of post-fire debris flows in the San Gabriel Mountains, CA, U.S.A., in *Debris-Flow Hazards Mitigation, Mechanics, Prediction, and Assessment*, edited by R. Genevois, D. L. Hamilton, and A. Prestininzi, pp. 583–593, Casa Ed. Univ. La Sapienza, Rome, doi:10.4408/IJEGE.2011-03.B-064.

Scott, D. F. (1993), The hydrological effects of fire in South African mountain catchments, *J. Hydrol.*, *150*, 409–432.

Sheridan, G. J., P. N. J. Lane, and P. J. Noske (2007), Quantification of hillslope runoff and erosion processes before and after wildfire in a wet eucalyptus forest, *J. Hydrol.*, *343*, 12–28, doi:10.1016/j.jhydrol.2007.06.005.

Sherman, L. K. (1932), The relation of hydrographs of runoff to size and character of drainage basins, *Eos Trans. AGU*, *13*, 332–339.

Smith, H. G., G. J. Sheridan, P. N. J. Lane, and L. J. Bren (2011), Wildfire and salvage harvesting effects on runoff generation and sediment exports from radiate pine and eucalypt forest catchments, south-eastern Australia, *For. Ecol. Manage.*, *261*, 570–581, doi:10.1016/j.foreco.2010.11.009.

Wilson, C. J. (1999), Effects of logging and fire on runoff and erosion on highly erodible granitic soils in Tasmania, *Water Resour. Res.*, *35*(11), 3531–3546.

J. E. Gartner, J. W. Kean, and D. M. Staley, U.S. Geological Survey, Box 25046, Denver Federal Center, Denver, CO 80225, USA. (jwkean@usgs.gov)

R. J. Leeper, U.S. Geological Survey, 525 S. Wilson Ave., Pasadena, CA 91106, USA.

K. M. Schmidt, U.S. Geological Survey, 345 Middlefield Rd., Menlo Park, CA 94025, USA.